



Characterization of coupling efficiency of silicon microring resonator using add-drop filter model

Mohammad Istiaque Reja^{1,2}

Received: 30 March 2018 / Accepted: 23 July 2018 / Published online: 2 August 2018
© The Optical Society of Japan 2018

Abstract

This paper presents a way of accurate characterization of the coupling efficiency of silicon microring resonator through curve fitting approach using an add-drop filter model which considers not only the waveguide propagation loss but also the backscattering effect due to sidewall roughness. The effective coupling efficiencies for different coupling angles from five differently positioned chips of two wafers are measured by comparing the experimental curve with the theoretical fit obtained from the developed model. The comparison of the results from this model with the Finite-Difference Time-Domain (FDTD) simulation results shows that the discrepancies increase with larger coupling angle i.e. larger coupling length, since longer couplers are more sensitive to the fabrication inaccuracies. The results found in this paper can serve as a good design tool in future to streamline the design of microring based structures on the same technological process.

Keywords Add-drop filter · All-optical NoC · Backscattering · Coupling efficiency · Microring resonator · Reflectivity · Waveguide loss

1 Introduction

The on-chip interconnection network or Network-on-Chip (NoC) is exploiting photonic solution as opposed to its electrical counterparts, especially in the multicore scenario where, in order to provide energy efficient performance with low latency and high throughput [1–5], one of the most promising technology is Silicon-On-Insulator (SOI) platform due to its compatibility with CMOS technology and high refractive index contrast [5–8].

An important element of integrated optical device is microring resonator which can be used as filter, modulator etc. Microring can also be used to create a NoC as proposed in [1] avoiding any waveguide crossings thus reducing crosstalk. Many methods have been proposed to improve the performances of

crossings based on multimode interference [9], mode expansion [10, 11], polymer waveguide bridges [12], Bloch waves [13] etc. [14]. Although the amount of crosstalk of single waveguide crossing can be reduced to as low as -20 dB [15], it can be substantially large in an optical NoC where multiple waveguide intersections are needed, and thus seriously degrade the signal quality. The use of Multi Micro Ring (MMR) structure in the all-optical NoC reported in [1] is a feasible solution to this problem which avoids the waveguide crossings completely.

With the increasing complexity of the device designs and increasing density of the functions integrated onto a single device, the characterization of the building blocks of all-optical Network-on-Chip (NoC) are becoming important to highlight the discrepancies between the fabrication outcome and the intended design [16]. The importance of accurate characterization lies in the fact that it allows to understand the tolerances of the fabrication process and the results found during the characterization stage can be used to mitigate the effect of fabrication inaccuracies by optimizing the design afterwards [17].

This paper presents an unique add-drop filter model to characterize the microring coupling efficiency by way of curve fitting. The novelty of this model lies in the fact that, unlike other models, it measures the effective coupling efficiency very precisely considering both the waveguide propagation loss and backscattering effect due to sidewall roughness.

Electronic supplementary material The online version of this article (<https://doi.org/10.1007/s10043-018-0450-3>) contains supplementary material, which is available to authorized users.

✉ Mohammad Istiaque Reja
istiaque@cuet.ac.bd

¹ Department of Electrical and Electronic Engineering, Chittagong University of Engineering and Technology, Chittagong 4349, Bangladesh

² Scuola Superiore Sant'Anna, 56124 Pisa, Italy

Comparing the experimental curve with the theoretical fit obtained from the model the effective coupling efficiency for different coupling angles from five differently positioned chips of two wafers are measured to verify the reliability of the chosen coupling angle for the required effective coupling efficiency in Multi Micro Ring (MMR) NoC reported in [1, 5]. Then the measured values are compared with the results obtained in the design phase using Finite Difference Time Domain (FDTD) simulation, to estimate the fabrication inaccuracies.

Little et al. developed an add-drop filter model in [18] considering the backscattering effect, but the authors didn't consider the waveguide propagation loss, whereas this model considers both the loss and backscattering effect due to sidewall roughness.

2 Microring coupling efficiency characterization

2.1 Add-Drop filter model

The all-pass filter model described in [19] is extended here for add-drop filter configuration shown in Fig. 1. To account for the backscattering, this model considers bidirectional propagation both in the bus and the ring as opposed to the usual model of [20, 21] where only unidirectional mode of the resonator is considered.

Such a system is described by an 8×8 scattering matrix:

$$\begin{bmatrix} A_1^- \\ A_2^- \\ A_3^- \\ A_4^- \\ A_5^- \\ A_6^- \\ A_7^- \\ A_8^- \end{bmatrix} = \begin{bmatrix} 0 & 0 & t_1 & ik_1 & 0 & 0 & 0 & 0 \\ 0 & 0 & ik_1 & t_1 & 0 & 0 & 0 & 0 \\ t_1 & ik_1 & 0 & 0 & 0 & 0 & 0 & 0 \\ ik_1 & t_1 & 0 & 0 & 0 & 0 & 0 & 0 \\ 0 & 0 & 0 & 0 & 0 & 0 & t_2 & ik_2 \\ 0 & 0 & 0 & 0 & 0 & 0 & ik_2 & t_2 \\ 0 & 0 & 0 & 0 & t_2 & ik_2 & 0 & 0 \\ 0 & 0 & 0 & 0 & ik_2 & t_2 & 0 & 0 \end{bmatrix} \begin{bmatrix} A_1^+ \\ A_2^+ \\ A_3^+ \\ A_4^+ \\ A_5^+ \\ A_6^+ \\ A_7^+ \\ A_8^+ \end{bmatrix} \quad (1)$$

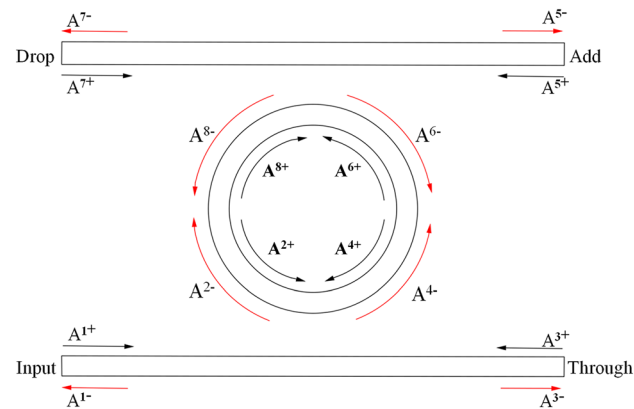


Fig. 1 Add-drop filter model

Here, A_i^+ ($i = 1, 2, \dots, 8$) and A_j^- ($j = 1, 2, \dots, 8$) are the eight inputs and eight outputs, respectively. The real coefficients κ_1, κ_2 and t_1, t_2 denotes the field coupling from bus to ring and field transmission respectively. The relation between these coefficients are $t_1^2 + \kappa_1^2 = 1$ and $t_2^2 + \kappa_2^2 = 1$ for lossless coupling. We have assumed here that both the directional couplers are identical, so $\kappa_1 = \kappa_2$ and $t_1 = t_2$. The ring feedback equations are expressed as follows:

$$\begin{aligned} A_2^+ &= aA_8^- e^{-i\delta} + R_c A_2^-; \\ A_4^+ &= aA_6^- e^{-i\delta} + R_c A_4^-; \\ A_6^+ &= aA_4^- e^{-i\delta} + R_c A_6^-; \\ A_8^+ &= aA_2^- e^{-i\delta} + R_c A_8^-; \end{aligned} \quad (2)$$

where δ and a are the accumulation of phase and field loss over half round trip, respectively, and they are expressed as $\delta = \text{optical length of half round} \times \frac{2\pi}{\lambda} = \pi r n_{\text{eff}} \times \frac{2\pi}{\lambda}$ and $a = e^{-\pi r \frac{\alpha}{2}}$, where r is the ring radius, α is the loss in dB/cm, n_{eff} is the effective refractive index. The reflection coefficient R_c is expressed as $R_c = Re^{i\gamma}$, where R is the reflectivity or backscattering and γ is the phase of R_c . The detail about these parameters can be found in [18, 19]

The transfer matrix of the add-drop filter obtained by solving the scattering matrix of Eq. (1) and ring feedback equations of Eq. (2) for $A_3^+ = 0$ and $A_7^+ = 0$ is as follows:

$$\begin{bmatrix} A_3^- \\ A_7^- \end{bmatrix} = \begin{bmatrix} t_1 - \frac{\kappa_1^2 F_8}{1 - F_8 t_1} & \frac{ik_1 F_7}{1 - F_8 t_1} \\ \frac{ik_2 F_7'}{1 - F_8' t_2} & t_2 - \frac{\kappa_2^2 F_8'}{1 - F_8' t_2} \end{bmatrix} \begin{bmatrix} A_1^+ \\ A_5^+ \end{bmatrix} \quad (3)$$

In this equation,

$$\begin{aligned} F_7 &= F_4 + \frac{F_5 F_2}{F_3}; F_8 = \frac{F_5 F_1}{F_3} + F_6; \\ F_7' &= F_4' + \frac{F_5' F_2'}{F_3'}; F_8' = \frac{F_5' F_1'}{F_3'} + F_6'. \end{aligned} \quad (4)$$

where

$$\begin{aligned} F_1 &= ae^{-i\delta} + \frac{aR_c^2 t_1 t_2 e^{-i\delta}}{F}; \\ F_2 &= R_c^2 t_2 ik_2 + \frac{a^2 R_c^2 t_1 t_2^2 e^{-2i\delta} ik_2}{F}; \\ F_3 &= 1 - R_c^2 t_2^2 - \frac{a^2 R_c^2 t_1 t_2^3 e^{-2i\delta}}{F}; \\ F_4 &= ae^{-i\delta} ik_2 + \frac{aR_c^2 t_1 t_2 e^{-i\delta} ik_2}{F}; \\ F_5 &= ae^{-i\delta} t_2 + \frac{aR_c^2 t_1 t_2^2 e^{-i\delta}}{F}; \\ F_6 &= \frac{R_c^2 t_1}{F}; \\ F &= 1 - a^2 t_1 t_2 e^{-2i\delta}. \end{aligned}$$

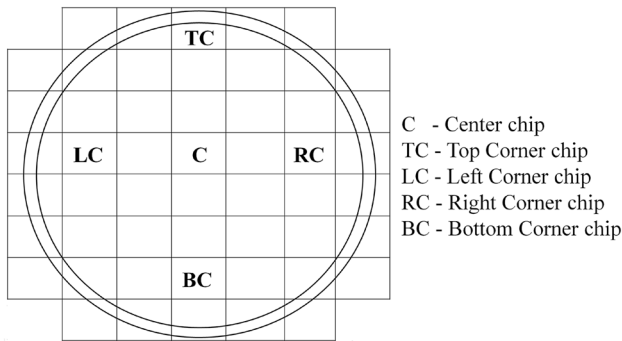


Fig. 2 The position of the characterized chips on the wafer

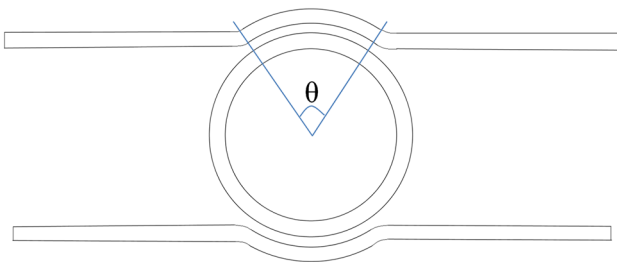


Fig. 3 An add-drop filter having bent bus waveguides

F'_1 to F'_6 can be found from F_1 to F_6 by replacing t_1 by t_2 and t_2 by t_1 and by replacing κ_1 by κ_2 and κ_2 by κ_1 .

Through fitting the drop port simulated spectrum (obtained from the above model) with the drop port experimental spectrum the coupling efficiency between the bus and ring waveguide of the microring can be measured.

2.2 Position of the characterized chips

Five differently positioned chips are selected from two different wafers for characterization. One center chip and four

corner chips are chosen as shown in Fig. 2. The measurements and the analysis of all these differently positioned chips will allow to find out the wafer scale uniformity of ring coupling efficiency across two wafers. In a multiproject wafer full-active run the chips were manufactured by IME through CMC microsystem.

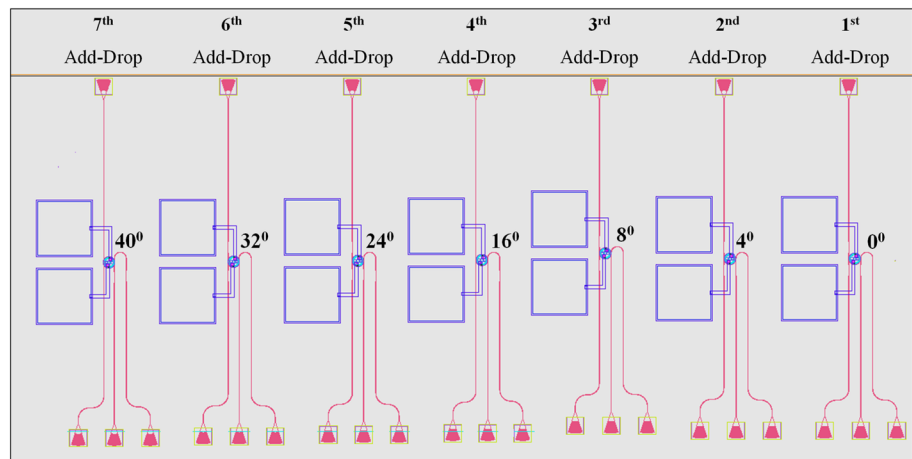
2.3 Device architecture and design

Figure 3 shows an add-drop filter where the coupling region is extended following the ring shape i.e. unlike usual straight bus waveguide, here the bus waveguide has a bending. This bending creates an arc that subtends an angle θ at the center of the ring. The more the arc length increases i.e. the angle increases, the more the coupling region will be extended which will result in a higher coupling efficiency. The angle θ is called as 'coupling angle'. To test the model, multiple add-drop rings with different coupling angles have been realized and characterized.

The fabricated PIC that contains the Multi Micro Ming (MMR) architecture based Network-on-Chip (NoC) has seven add-drop filters of different coupling angles in order to characterize the effective coupling efficiency after the fabrication. The coupling angles of these seven add-drop filters are 0° , 4° , 8° , 16° , 24° , 32° , 40° from right to left respectively as shown in the mask image of Fig. 4. Figure 5 shows one add-drop filter from the mask separately where the position of the ports of the add-drop filter are specified.

The cross-section of the bus and ring in the coupling region are schematically shown in Fig. 6. The cross-section of the bus consists of a single-mode channel waveguide (with embedded core) having a width of 460 nm and a height of 220 nm, whereas the cross-section of the ring consists of a single-mode half-rib waveguide having a width of 480 nm and height of 220 nm. A 90 nm thick internal slab of doped silicon is placed 1 μm away from the microring waveguide

Fig. 4 Mask image of seven add-drop filters having bent bus waveguides of different angles



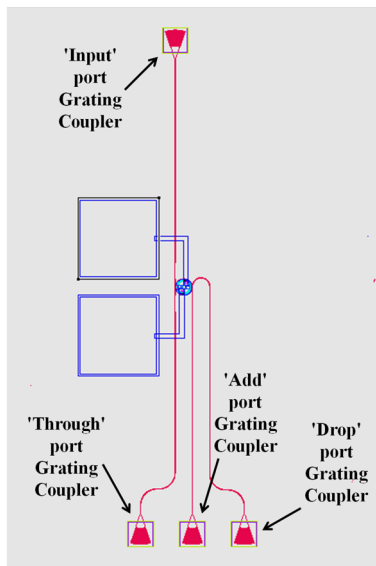


Fig. 5 Mask image of an add-drop filter showing the position of the ports

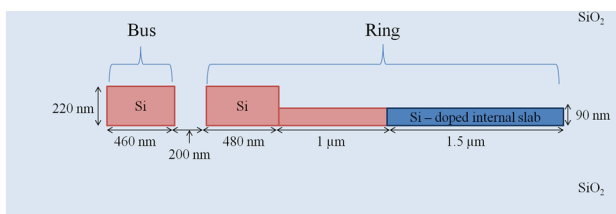


Fig. 6 Device cross-section in the coupling region

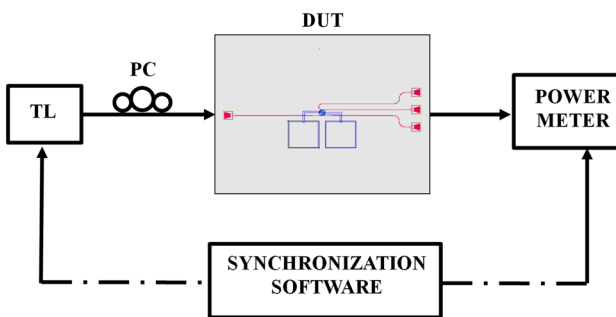


Fig. 7 Experimental setup

to tune the rings independently by exploiting the Joule effect through electrical current injection in this doped region.

2.4 Experimental measurement

The schematic diagram of the experimental setup is shown in Fig. 7. Spectral scans are taken using an external cavity Tunable Laser (TL) by generating a continuous wave signal

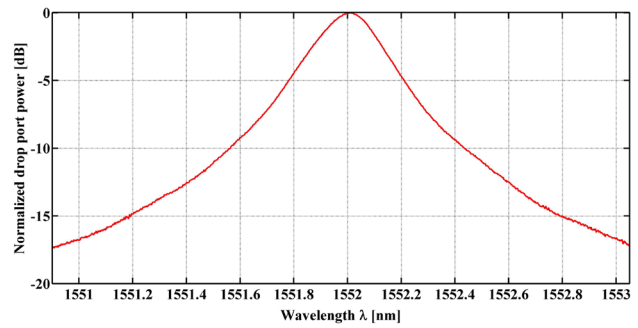


Fig. 8 A selected resonance near 1550 nm from the measured drop port experimental curve for 32° coupling angle from the wafer 2 top corner chip

having 0 dBm power in the range of 1500–1600 nm. A fiber Polarization Controller (PC) maximizes the coupling efficiency between the optical fiber and the input grating coupler. The output spectrum is collected with a spectral resolution of 1 picometer from the ‘drop’ port grating coupler using a synchronized power meter. A temperature controller is used to maintain a constant temperature of 25 °C.

2.5 Characterization of microring coupling efficiency by curve fitting using the add-drop filter model

In this section, how to step by step fit the simulated curve obtained from the described add-drop filter model with the experimental curve from the drop port will be shown to measure the actual coupling efficiency. To illustrate this an add-drop filter having coupling angle of 32° is chosen from of the top corner chip of wafer 2.

Since our model use both the waveguide propagation loss and backscattering values for accurately characterizing the coupling efficiency, we need to measure these values beforehand. The different ways to measure the waveguide loss are compared in [22] and the method based on the all-pass filter model [19] is shown to be the most simple and accurate, because this method is independent of input coupling losses and estimation of facet reflectivity is not required here. So, using the model of [19], the waveguide propagation loss and backscattering values from all the differently positioned chips of both the wafers are measured and reported in [23]. For the top corner chip of wafer 2, the measured value of loss (α) = 2.55 dB/cm and backscattering (R) = 0.00425.

The step by step fitting is as follows:

- Step 1: A resonance near 1550 nm is selected from the experimental spectrum of the drop port which is shown in Fig. 8.
- Step 2: At first, both the loss (α) and backscattering (R) are considered as zero and by varying power coupling effi-

ciency $K (= \kappa^2)$ the simulated curve from the add-drop model is fitted with experimental spectrum.

Step 3: After that the actual loss value for this chip i.e. loss (α) = 2.55 dB/cm is considered keeping the backscattering (R) value to be still zero. Loss will decrease the peak of the simulated curve. If we normalize it to compare both the curves, bandwidth of the simulated curve will change. So, to fit with the experimental curve we need to decrease the value of K .

Step 4: Finally the actual value of both the loss and backscattering for this chip i.e. loss (α) = 2.55 dB/cm and backscattering (R) = 0.00425 are considered. Backscattering will again decrease the peak of the simulated curve. After the normalization the bandwidth of the simulated curve will change and we need to decrease the value of K to fit with the experimental curve. For (K) = 8.38% both the curves match properly as shown in Fig. 9.

So, in wafer 2 top corner chip the value of coupling efficiency for 32° coupling angle is found to be 8.38%.

Figure 10 shows another example of fitting for 24° coupling angle from wafer 2 center chip. For this chip the loss and backscattering were found to be 3.1 dB/cm and 0.00505 respectively as reported in [23]. From Fig. 10 it can be seen that for coupling efficiency of 4.84% the simulated and experimental curves match properly.

In both the examples, the backscattering values are small (less than 0.005) and can be negligible. However, if the value is higher it can reduce the effective coupling efficiency significantly. For example, in the first case i.e. for 24° coupling angle of wafer 2 top corner chip, if the backscattering value would be 0.0101 instead of 0.00425, the effective coupling efficiency would reduce to 7.802% from 8.38%.

By following the above mentioned approach the experimentally measured spectra from the drop ports of all the add-drop filters (having different coupling angles) of five

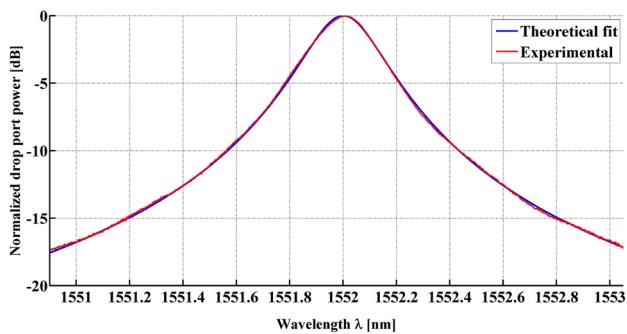


Fig. 9 The measured drop port experimental curve for 32° coupling angle from wafer 2 top corner chip and the theoretical fit obtained from the add-drop model using loss (α) = 2.55 dB/cm, backscattering (R) = 0.00425 and power coupling efficiency (K) = 8.38%

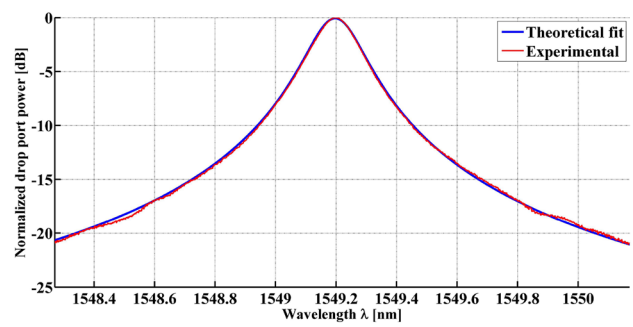


Fig. 10 The measured drop port experimental curve for 24° coupling angle from wafer 2 center chip and the theoretical fit obtained from the add-drop model using loss (α) = 3.1 dB/cm, backscattering (R) = 0.00505 and power coupling efficiency (K) = 4.84%

differently positioned chips fabricated from two wafers are fitted with the simulated curve, and thus their effective coupling efficiencies are measured and shown in Fig. 11. This figure also shows the coupling efficiency variations across two wafers i.e. wafer 1 (W1) and wafer 2 (W2).

2.6 Comparison with the FDTD simulation results

Table 1 shows the comparison between the coupling efficiency values found using Finite-Difference Time-Domain (FDTD) simulation and from the add-drop filter model. For both the wafers the average values of coupling efficiencies from five different positioned chips for different coupling angles are shown. The FDTD simulations have been done for a directional coupler having the same cross section of the coupling region present on the fabricated PIC i.e. the ring width of 480 nm and bus width of 460 nm with a bus to ring gap of 200 nm.

In Fig. 12 the plot of the discrepancy between these two results with the coupling angle for both the wafers are shown. From this figure, we can see that for both the wafers

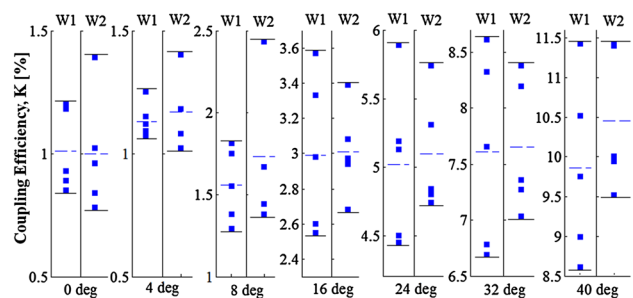
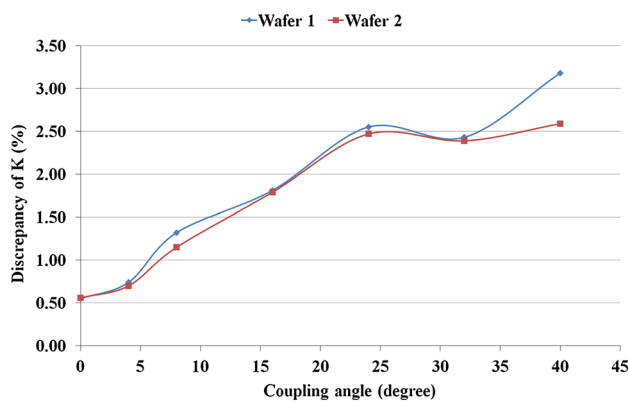


Fig. 11 Variation of the coupling efficiency values across two wafers measured from five differently positioned chips for coupling angle of 0°, 4°, 8°, 16°, 24°, 32°, 40°. For each dataset the upper line denotes the maximum, lower line denotes the minimum, and middle dotted line denotes the average coupling efficiency

Table 1 Comparison between the coupling efficiency values found using FDTD simulation and using add-drop model

Coupling angle (°)	Coupling efficiency, K (%)		
	Using FDTD simulation	Using the add-drop model	
		Average value from 5 differently positioned chips of wafer 1	Average value from 5 differently positioned chips of wafer 2
0	1.56	1.01	1.00
4	1.87	1.13	1.17
8	2.88	1.56	1.73
16	4.80	2.99	3.01
24	7.57	5.02	5.10
32	10.04	7.61	7.65
40	13.04	9.86	10.45

**Fig. 12** The plot of discrepancy (between the results of K found from the FDTD simulation and from the add-drop filter model) with the coupling angle in wafer 1 and wafer 2

the discrepancies from the FDTD simulation results at different coupling angles are almost identical. So, we can say that both the wafers have uniform characteristics in terms of their effective coupling efficiencies due to the uniform fabrication outcomes. Also it can be noticed from the Fig. 12 that with the increasing coupling angle the discrepancy in both the wafer increases. This effect is related to the increment of the coupling length and longer couplers are more sensitive to the fabrication inaccuracy.

The required coupling efficiency for the proposed NoC reported in [1, 5] is 7.5% to guarantee the transmission BW for a 10 Gbs non return-to-zero on-off keyed signal. As can be seen from the FDTD simulation results (reported in Table 1), 24° coupling angle could be exploited to achieve 7.5% coupling efficiency. But 32° coupling angle was chosen instead to counteract the effect of the fabrication inaccuracies. We can see from Table 1 that the average effective coupling efficiency values in wafer 1 and wafer 2 for 32° coupling angle are 7.61 and 7.65, respectively, instead of 10%. So, the result from the add-drop model verifies that 32° coupling angle was appropriately chosen in [1, 5] to provide

the required coupling efficiency for the MMR architecture based NoC.

The results of the effective coupling efficiency values for different coupling angles found from the developed add-drop model will serve as a very good design tool in future, as this model provide the effective coupling efficiency value very precisely considering not only the effect of waveguide propagation loss but also the backscattering effect.

On the other hand, the FDTD simulation, although being a valuable and flexible design tool, is very time and resource consuming. For this reason just the coupling region is typically simulated (not the entire add-drop microring). Also the fabrication process inaccuracies can not be considered.

The results from the developed model give an idea of the discrepancy range of the coupling efficiency values due to the fabrication inaccuracies which will help the designer to choose the appropriate coupling angle to achieve desired coupling efficiency.

3 Conclusion

An add-drop filter model in order to precisely characterize the effective coupling efficiency considering both the loss and backscattering effects is presented in this paper. The effective coupling efficiency values found for different coupling angles (from five differently positioned chips of two wafers) using the developed model will serve as a very good design tool in future to streamline the design of microring based structures on the same technological process. The results verified that 32° coupling angle is appropriately chosen in order to get minimum 7.5% effective coupling efficiency for the Multi Micro Ring (MMR) architecture based NoC reported in [1, 5]. Furthermore, the results are compared with the Finite-Difference Time-Domain (FDTD) simulation results which allows to measure the discrepancies from the design values due to the fabrication inaccuracies. It is expectedly found that the discrepancies increase

with larger coupling angle, since longer couplers are more sensitive to the fabrication inaccuracies. It is also found that the discrepancies at different coupling angles are almost identical for both the wafers due to the uniform fabrication outcomes.

Acknowledgements The author would like to sincerely thank Dr. Nicola Andriolli (Assistant Professor, Scuola Superiore Sant'Anna, Italy) and Fabrizio Gambini (Researcher, CNIT-National Laboratory of Photonic Networks, Pisa, Italy) for their technical support, valuable suggestions and feedbacks throughout this work. The author would also like to thank the Institute of Microelectronics (IME), Singapore and CMC Microsystems for the foundry service.

Compliance with ethical standards

Conflict of interest The author states that there is no conflict of interest.

References

- Pintus, P., Contu, P., Raponi, P., Cerutti, I., Andriolli, N.: Silicon-based all-optical multi microring network-on-chip. *Opt. Lett.* **39**(4), 797–800 (2014)
- Gambini, F., Pintus, P., Faralli, S., Chiesa, M., Preve, G.B., Cerutti, I., Andriolli, N.: Experimental demonstration of a 24-port packaged multi-microring network-on-chip in silicon photonic platform. *Opt. Express* **25**(18), 22004–22016 (2017)
- Wang, X., Gu, H., Yang, Y., Wang, K., Hao, Q.: Rpnoc: a ring-based packet-switched optical network-on-chip. *IEEE Photon. Technol. Lett.* **27**(4), 423–426 (2015)
- Shacham, A., Bergman, K., Carloni, L.P.: Maximizing gops-per-watt: high-bandwidth, low power photonic on-chip networks. In: *Proceedings of Third Watson Conference on Interaction between Architecture, Circuits, and Compilers*, p. 1221 (2006)
- Gambini, F., Faralli, S., Pintus, P., Andriolli, N., Cerutti, I.: BER evaluation of a low-crosstalk silicon integrated multi-microring network-on-chip. *Opt. Express* **23**(13), 17169–17178 (2015)
- Bogaerts, W., et al.: Silicon microring resonators. *Laser Photon. Rev.* **6**(1), 4773 (2012)
- Doylend, J.K., Knights, A.P.: The evolution of silicon photonics as an enabling technology for optical interconnection. *Laser Photon. Rev.* **6**(4), 504–525 (2012)
- Ma, Y., et al.: Ultralow loss single layer submicron silicon waveguide crossing for SOI optical interconnect. *Opt. Express* **21**(24), 29374–23982 (2013)
- Luo, Y., et al.: Low-loss low-crosstalk silicon rib waveguide crossing with tapered multimode-interference design. In: *Proceedings of IEEE 9th International Conference on Group IV Photonics (GFP)*, pp. 150–152 (2012)
- Zhang, Y., Yang, S., Lim, A.E., Lo, G.Q., Galland, C., Baehr-Jones, T., Hochberg, M.A.: CMOS-compatible, low-loss, and low-crosstalk silicon waveguide crossing. *IEEE Photon. Technol. Lett.* **25**(5), 422–425 (2013)
- Chen, L., Chen, Y.K.: Compact, low-loss and low-power 8×8 broadband silicon optical switch. *Opt. Express* **20**(17), 18977–85 (2012)
- Tsarev, A.V.: Efficient silicon wire waveguide crossing with negligible loss and crosstalk. *Opt. Express* **19**(15), 13732–13737 (2011)
- Zhang, Y., Hosseini, A., Xu, X., Kwong, D., Chen, R.T.: Ultralow-loss silicon waveguide crossing using Bloch modes in index-engineered cascaded multimode-interference couplers. *Opt. Lett.* **38**(18), 3608–3611 (2013)
- Ma, Y., et al.: Ultralow loss single layer submicron silicon waveguide crossing for SOI optical interconnect. *Opt. Express* **21**(24), 29374–82 (2013)
- Sherwood-Droz, N., Wang, H., Chen, L., Lee, B.G., Biberman, A., Bergman, K., Lipson, M.: Optical 4×4 hitless silicon router for optical networks-on-chip (NoC). *Opt. Express* **16**(20), 15915–15922 (2008)
- Kuramochi, E., et al.: Large-scale integration of wavelength-addressable all-optical memories on a photonic crystal chip. *Nat. Photon.* **8**, 474–481 (2014)
- Bruck, R., et al.: Device-level characterization of the flow of light in integrated photonic circuits using ultrafast photo modulation spectroscopy. *Nat. Photon.* **9**, 5460 (2015)
- Little, B.E., Laine, J.P., Chu, S.T.: Surface-roughness-induced contradirectional coupling in ring and disk resonators. *Opt. Lett.* **22**(1), 46 (1997)
- Moresco, M., et al.: Method for characterization of Si waveguide propagation loss. *Opt. Express* **21**(5), 5391–5400 (2013)
- Yariv, A.: Universal relations for coupling of optical power between microresonators and dielectric waveguides. *Electron. Lett.* **36**(4), 321322 (2000)
- Heebner, J., Grover, R., Ibrahim, T.: *Optical Microresonator: Theory, Fabrication and Application*. Springer Series in Optical Sciences (**ISBN: 978-0-387-73068-4**)
- Reja, M.I., et al.: A comparative analysis of the characterization methods for submicron silicon waveguide propagation loss. In: *Proceedings of 2nd International Conference on Electrical Information and Communication Technologies (EICT)*, pp. 347–352 (2015)
- Reja, M.I.: Intra- and inter-wafer characterization of waveguide propagation loss and reflectivity. In: *Proceedings of IEEE International Conference of Telecommunication and Photonics (ICTP)*, pp. 1–5 (2015)